Supramolecular Complex Coupled to a Metal Nanoparticle: Computational Studies on the Optical Absorption

ARTICLE *in* THE JOURNAL OF PHYSICAL CHEMISTRY A · JUNE 2012

Impact Factor: 2.69 · DOI: 10.1021/jp305505c · Source: PubMed

3 AUTHORS, INCLUDING:

Yaroslav Zelinskyy
Humboldt-Universität zu Berlin
19 PUBLICATIONS **135** CITATIONS
SEE PROFILE

Yuan Zhang
Humboldt-Universität zu Berlin
8 PUBLICATIONS **39** CITATIONS
SEE PROFILE

THE JOURNAL OF PHYSICAL CHEMISTRY A

Article

pubs.acs.org/JPCA

Supramolecular Complex Coupled to a Metal Nanoparticle: Computational Studies on the Optical Absorption

Yaroslav Zelinskyy,[†,‡] Yuan Zhang,[†] and Volkhard May*[,†]

[†]Institut für Physik, Humboldt-Universitäat zu Berlin, Newtonstraße 15, D-12489 Berlin, Germany

[‡]Bogolyubov Institute for Theoretical Physics, National Academy of Sciences of Ukraine, Metrologichna str., 14-b, UA-03143 Kiev, Ukraine

ABSTRACT: Absorption spectra of a supramolecular complex (SC) placed in the proximity of a spherical metal nanoparticle (MNP) are computed. A description of the absorption is used that is based on a density matrix propagation. The applied density matrix theory starts from a microscopic model including the Coulomb interaction between the SC and the MNP. This interaction is dominated by an energy exchange coupling between the excitations of the SC and the multipolar excitations of the MNP. Its nonperturbative consideration results in a shift and a broadening of all Frenkel-exciton levels as well as an oscillator strength change. If a J-aggregate type SC near a MNP is considered, all exciton levels strongly contribute to the absorption what is in contrast to the isolated SC.

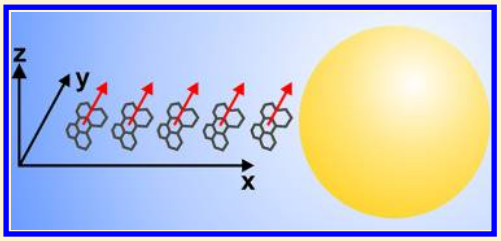

I. INTRODUCTION

The knowledge of the optical absorption of a molecular system represents one basic prerequisite for a proper application of all up to date ultrafast and nonlinear spectroscopic techniques. For example, the correct interpretation of femtosecond transient absorption spectra displaying quantum mechanical wave packet dynamics is based on the frequency domain linear absorption spectrum. Interestingly, there is also a nice interrelation in theory between the frequency-domain absorption spectra and real time ultrafast phenomena. This interrelation concerns the determination of the molecular system's absorption by the time propagation of a particular wave function. It was E. J. Heller who first indicated this more than three decades ago.[1]

Introducing the absorption line shape $I(\omega)$ via the formula $\alpha(\omega) = 4\pi\omega n I(\omega)/\hbar c$, where $\alpha(\omega)$ is the absorption coefficient and n the volume density of absorbing units, one obtains for the absorption line shape of a molecule:[2]

$$I(\omega) = \frac{1}{3}|d_{eg}|^2 Re \int_0^\infty dt\ e^{i(\omega+E_{g0}/\hbar)t}\langle\chi_{g0}|e^{-iH_e t/\hbar}|\chi_{g0}\rangle \quad (1)$$

d_{eg} denotes the electronic transition dipole moment between the electronic ground state φ_g and the excited state φ_e, and χ_{g0} is the vibrational ground-state wave function in the electronic ground state. The formula displays the representation of the frequency dependent absorption line shape as the Fourier transform of a wave function correlation function. The latter relates the initial vibrational state χ_{g0} to its time propagation in the excited state according to $\exp(-iH_e t/\hbar)\chi_{g0}$ (the vibrational Hamiltonian in the excited electronic state is given by H_e). In this way, an absorption formula of Fermi's Golden Rule type, which includes summations with respect to vibrational eigenstates in the ground and excited electronic state, is replaced by a wave function propagation at the excited-state potential energy surface (PES). Because expression 1 does not converge, it needs the inclusion of a time cutoff, for example, by including the exponential decaying factor $\exp(-\gamma t)$. Usually, this is identified by a dephasing between the two involved electronic states. Dephasing is automatically included if eq 1 is generalized to an open system description, i.e., to molecular systems feeling the presence of a certain environment.[2,3]

It is just the aim of the following discussion to demonstrate a particular use of this extension. Therefore, we will compute the absorption line shape of a supramolecular complex (SC) in the close vicinity of a metal nanoparticle (MNP). Collective plasmon excitations of the MNP electrons have to be expected to strongly enhance the SC absorption. This observation is of particular interest in the tremendously growing field of plasmonics.[4,5]

Besides many experiments focusing on photoemission spectra, attempts have been also reported on the measurement of extinction (absorption) spectra. Layers of organic molecules deposited on metal films or nanostructured metal surfaces were studied in refs 6−8. The coupling of Frenkel excitons (formed in the molecular layers) to surface plasmons of the metal was demonstrated. Absorption spectra of spherical gold and silver MNP coated with dye aggregates (cyanine derivatives) have been measured in refs 9−11, indicating a mixed absorption due to MNP and exciton contributions. Some first hints on such absorption changes could be also reported in ref 12 where the absorbance of a silver nanowire encapsulated by a cyanine dye tubular aggregate was detected. An enhancement of chlorophyll absorption upon the presence of a MNP was measured in ref 13 by attaching the photosynthetic protein complex PS1 to the

Special Issue: Jörn Manz Festschrift

Received: June 5, 2012
Revised: June 26, 2012
Published: June 26, 2012

surface of silver and gold spherical MNPs. Related theoretical descriptions of the Frenkel-exciton system are mainly based on the use of a single-resonance dielectric function.[9−11,14] In refs 15 and 16 an ensemble of dipoles surrounding a spherical MNP was simulated introducing a classical description of the dipoles (which carry out harmonic oscillations driven by the surrounding electromagnetic field) and by constructing a solution of Maxwell's equations.

In the present contribution we study an interacting SC−MNP system as shown in Figure 1. Such an arrangement of a strictly linear SC and a spherical MNP placed on a nonconducting surface, for example, has not been studied in the experiment so far. However, there are several recent reports on a spectroscopic characterization of single polymeric chains showing the formation of Frenkel-exciton states. Nanofibers of poly(3-hexylthiophene) with single-chain J-aggregate character have been studied in ref 17. Coherent control experiments could be performed with an organic quantum wire built by a single polydiacetylene chain.[18] A description of exciton formation in different self-assembled zinc *meso*-tetra(4-pyridyl)-porphyrin aggregates can be found in ref 19. And, exciton−exciton annihilation dynamics in perylene bisimide J-aggregates were reported in ref 20. So, it would be appropriate to study such systems placed in the vicinity of a MNP. Because Frenkel-exciton states formed in a linear SC are characterized by particular selection rules (a J-aggregate absorption, for example, is dominated by the lowest exciton level), the coupling to a MNP may change these rules. It is just this point we will address in the following.

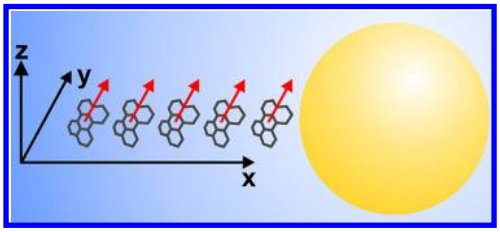

Figure 1. Scheme of the considered SC−MNP system. The molecules (here perylene with transition dipole moments drawn as red arrows) are assumed to form a linear SC placed in the vicinity of a spherical MNP.

To do this, we introduce a complete quantum description of the SC−MNP system. Because the spatial extension of the SC−MNP system we will study is much less than the wavelengths corresponding to characteristic photon energies, a description via instantaneous (longitudinal) Coulomb forces becomes possible. Some first work in this line has been already presented recently by us in refs 21−23. There, a microscopic description of a molecule−MNP system could be carried out on the basis of the inclusion of that part of the Coulomb coupling, which is responsible for excitation energy exchange. Its nonperturbative account results in a level shift and broadening as well as oscillator strength redistribution of a single molecule or a SC. The approach is beyond the mean-field description of the SC−MNP Coulomb coupling, which is automatically chosen when a local field formed due to the presence of the MNP is introduced (see also the recent remarks on this problem in ref 24). The present work introduces the essential extension of our former simulations in ref 22 by including all multipole surface plasmon excitations which appear in a spherical MNP. Though this is of no importance for the absorption line shape, it basically influences the energy exchange coupling between the SC and the MNP.

The paper is organized as follows. In the next section we offer a brief motivation of the model including the construction of the MNP Hamiltonian accounting for multipole excitations. Some remarks on the used density matrix theory are also given. Section III shortly describes the computation of the absorption via a density matrix propagation. Our numerical results are collected in section IV. The paper ends with some concluding remarks. More detailed considerations are collected in the appendices.

II. THE SC−MNP MODEL AND DENSITY MATRIX EQUATIONS

A. SC Hamiltonian. We start by characterizing the molecules forming the SC. Their description is reduced to the electronic ground state φ_{ng} and the first excited state φ_{ne} (n counts the molecules in the chain). The related energies are E_{ng} and E_{ne}, respectively. It is suitable to introduce an expansion of the total SC Hamiltonian with respect to the relevant electronic states. According to the present aims (computation of linear absorption spectra) only singly excited states of the SC (besides the ground state) are of interest. The system's ground state reads $|\phi_g\rangle = \prod_n|\varphi_{ng}\rangle$, and singly excited states correspond to $|\phi_n\rangle = |\varphi_{ne}\rangle\prod_{n'\neq n}|\varphi_{n'g}\rangle$. The reduction of the original Hamiltonian to its electronic ground state and singly excited states is written as $H = H_0 + H_1$, where the Hamiltonian of the SC electronic ground state takes the form $H_0 = E_g|\phi_g\rangle\langle\phi_g|$ with $E_g = \sum_n E_{ng}$. The singly excited-state Hamiltonian of the SC follows as $H_1 = \sum_n(E_n + E_g)|\phi_n\rangle\langle\phi_n| + \sum_{n,n'}J_{nn'}|\phi_n\rangle\langle\phi_{n'}|$. The used representation of the Hamiltonian is often called *site representation*. The E_n are the molecular excitation energies $E_{ne} - E_{ng}$ and $J_{nn'}$ is the so-called excitonic coupling responsible for excitation energy transfer from molecule n to molecule n'. To introduce the exciton representation of H_1, we note that it can be diagonalized by introducing exciton states $|\alpha\rangle = \sum_n C_\alpha(n)|\phi_n\rangle$ with expansion coefficients $C_\alpha(n)$ and exciton energies E_α. It results in $H_1 = \sum_\alpha(E_\alpha + E_g)|\alpha\rangle\langle\alpha|$ (cf. also Figure 2).

B. MNP Plasmon Hamiltonian. If the SC is placed near a MNP, the MNP conduction band electrons may strongly interact with the various molecules of the SC. We chose a description where *collective plasmon excitations* directly couple

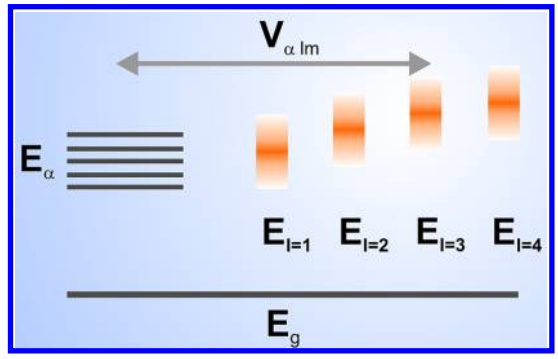

Figure 2. Energy level scheme of the SC−MNP system shown in Figure 1. The SC is represented by its exciton energies E_α (E_g denotes the SC−MNP ground-state energy). The multipole excitation energies E_l referring to the spherical MNP are drawn as broadened levels (orange) reflecting their short lifetime. They are connected with the exciton levels via the energy exchange coupling with matrix elements $V_{\alpha,lm}$.

dx.doi.org/10.1021/jp305505c | J. Phys. Chem. A 2012, 116, 11330−11340

to the electronic transitions in the SC. Individual electron−hole pair excitations complement the description by forming a reservoir, which is responsible for the nonradiative decay of the collective plasmon excitations. In particular, the approach is well suited to describe the coupling of the MNP to a larger SC. The problem we will address in the following is to find for the MNP electron Hamiltonian H_{MNP} an approximate representation like

$$H_{pl} = \sum_N E_N |N\rangle\langle N| \tag{2}$$

which concentrates on the collective plasmon excitations with energy E_N and state vector $|N\rangle$.

Focusing on a single conduction band of the MNP the standard notation of the MNP electron Hamiltonian is

$$H_{MNP} = \sum_j \frac{\mathbf{p}_j^2}{2m_{el}} + \frac{1}{2}\sum_{j,j'} \frac{e^2}{|\mathbf{x}_j - \mathbf{x}_{j'}|} + \sum_j v_{ion}(\mathbf{x}_j) \tag{3}$$

It describes the set of N_{el} conduction band electrons, includes the Coulomb coupling among them, and characterizes the effect of the metal ions by the local potential v_{ion}. The related MNP electron wave functions are denoted as $\psi_k(x)$ with quantum number k and with the set of electron coordinates x. The MNP electron eigenenergies E_k represent a broad continuum covering collective and individual excitations, i.e., surface plasmons, volume plasmons, and single electron−hole excitations.

The problem to move from the basic many-electron Hamiltonian, eq 3, to an approximate Hamiltonian, like in eq 2, displaying only a certain part of the whole spectrum has been solved in refs 26−28. By introducing the electron center of mass coordinate $\mathbf{R} = \sum_j \mathbf{x}_j/N_{el}$ as well as electron coordinates defined relative to $\mathbf{R}$, we could describe dipole plasmons of a spherical MNP. The finite plasmon lifetime could be computed. It originates by the coupling of the center of mass motion to the electron motion relative to the center of mass. Redefining the MNP Hamiltonian with the center of mass coordinate $\mathbf{R}$ it takes the form $H_{MNP} = H_{MNP}^{(rel)} + \hbar^2\nabla_{\mathbf{R}}^2/2N_{el}m_{el} + U(\mathbf{R},r)$, where $H_{MNP}^{(rel)}$ is identical with the expression in eq 3 but defined by electron coordinates relative to $\mathbf{R}$ (the whole set is denoted by r). We also introduced $U(\mathbf{R},r) = \sum_j (v_{ion}(\mathbf{R} + \mathbf{r}_j) - v_{ion}(\mathbf{r}_j))$. According to refs 26−28 a "plasmon" potential $U_{pl}(\mathbf{R}) = \langle\psi_0| U(\mathbf{R},r)|\psi_0\rangle$ can be defined by averaging $U(\mathbf{R},r)$ with respect to the ground-state wave function of relative electron motion. The potential is dominated by a second-order term $\sim\mathbf{R}^2$. Perturbation theory with respect to $U(\mathbf{R},r) - U_{pl}(\mathbf{R})$ results in rates of nonradiative plasmon decay.

We applied this approach in refs 21−23, but interestingly, it has been not used so far to describe higher multipole excitations of a spherical MNP. This inability may be caused by defining the "plasmon" potential $U_{pl}(\mathbf{R})$ exclusively by the ground-state electron wave function. However, there are other attempts which pave the way to an approximate MNP electron Hamiltonian like in eq 2. Details are quoted in Appendix A.

C. Molecule−MNP Coupling. Using the eigenstates of the MNP electron Hamiltonian, eq 3, the essential part of the Coulomb coupling between molecule n and the MNP reads

$$H_{Mol-MNP} = \sum_k V_{ne0,kng} |\varphi_{ne}\psi_0\rangle\langle\psi_k\varphi_{ng}| + \text{H.c.} \tag{4}$$

The expression describes excitation energy exchange between the MNP and the molecule. The MNP is de-excited from state ψ_k to its ground state ψ_0 while the molecule moves from the ground state φ_{ng} to the excited state φ_{ne}. The coupling matrix elements take the form (the y_u are the electron coordinates of molecule n):

$$V_{ne0,kng} = \langle\varphi_{ne}\psi_0| \sum_{j,u} \frac{e^2}{|\mathbf{x}_j - \mathbf{y}_u|} |\psi_k\varphi_{ng}\rangle = \int d^3\mathbf{x}\, d^3\mathbf{y}\, \frac{en_{k0}^*(\mathbf{x})\, en_{n,eg}(\mathbf{y})}{|\mathbf{x} - \mathbf{y}|} \tag{5}$$

A more compact notation is achieved in the second part of this equation where electronic transition densities are introduced. The MNP transition density reads $n_{k0}(\mathbf{x}) = N_{el}\int dx\ \delta(\mathbf{x} - \mathbf{x}_1)\psi^*_k(x)\ \psi_0(x)$. The one for the molecule looks similar. Moreover, an electrostatic type of coupling of the molecule to its own mirror charges induced in the MNP becomes also possible. It appears if the charge distribution of electrons and nuclei in the molecule (being either in its ground or in its excited state) stays locally uncompensated. We will assume, however, that this contribution is small.

Next we assume that a description of the molecular excitation in terms of the transition dipole moment $\mathbf{d}_n$ of molecule n is sufficient. Accordingly, the energy exchange coupling follows as

$$V_{ne0,kng} \approx -[\mathbf{d}_n\mathbf{E}_{k0}^*(\mathbf{X}_n)] \tag{6}$$

where we introduced the MNP induced electric field

$$\mathbf{E}_{k0}(\mathbf{X}_n) = -\nabla_{\mathbf{X}_n}\int d^3\mathbf{x}\, \frac{en_{k0}(\mathbf{x})}{|\mathbf{X}_n - \mathbf{x}|} \tag{7}$$

$\mathbf{X}_n$ is the center of mass distance between molecule n and the MNP.

D. Coupled SC−MNP System. As in the case of the SC Hamiltonian we restrict the description to the ground state and to the first excited states with either a single excitation in the SC or a single excitation of the MNP. The formulation of the Hamiltonian appears as a simple extension of what has been done to arrive at the SC Hamiltonian. We consider the MNP as a further excitable unit and introduce the ground state as $|\phi_g\rangle = \prod_n|\varphi_{ng}\rangle|0\rangle$, where $|0\rangle$ is the MNP electronic ground state. Singly excited states of the SC are $|\phi_n\rangle = |\varphi_{ne}\rangle\prod_{n'\neq n}|\varphi_{n'g}\rangle|0\rangle$. Those of the MNP can be denoted as $|\phi_N\rangle = \prod_n|\varphi_{ng}\rangle|N\rangle$ $(N > 0)$. The Hamiltonian of the SC−MNP electronic ground state is again written as the form $H_0 = E_g|\phi_g\rangle\langle\phi_g|$ but now with $E_g = \sum_g E_{ng} + E_0$. For the following, E_g is set zero and the singly-excited-state Hamiltonian of the SC−MNP system follows as

$$H_1 = \sum_n E_n|\phi_n\rangle\langle\phi_n| + \sum_{n,n'} J_{nn'}|\phi_n\rangle\langle\phi_{n'}| + \sum_N E_N|\phi_N\rangle\langle\phi_N| + \sum_{n,N}(V_{nN}|\phi_n\rangle\langle\phi_N| + \text{H.c.}) \tag{8}$$

The E_N represent excitation energies referring to the various collective MNP excitations. The molecule MNP excitation energy transfer coupling $V_{nN} \equiv V_{ne0,Nng}$, eq 5, accounts for deexcitation of the MNP and excitation of molecule n.

If the SC part is taken in the exciton representation, we get the singly-excited-state Hamiltonian of the SC−MNP system according to

dx.doi.org/10.1021/jp305505c | J. Phys. Chem. A 2012, 116, 11330−11340

$$H_1 = \sum_{\alpha} E_{\alpha}|\phi_{\alpha}\rangle\langle\phi_{\alpha}| + \sum_{N} E_N|\phi_N\rangle\langle\phi_N| + \sum_{\alpha,N} (V_{\alpha N}|\phi_{\alpha}\rangle\langle\phi_N| + \text{H.c.}) \tag{9}$$

with the states $|\phi_\alpha\rangle = |\alpha\rangle|0\rangle$ and with the exciton MNP interaction

$$V_{\alpha N} = \sum_{m} C_{\alpha}^{*}(m) V_{mN} \tag{10}$$

Figure 2 shows the ingredients of H_1, eq 9. Finally, it remains to quote the dipole operator of the SC−MNP system

$$\hat{\boldsymbol{\mu}} = \sum_{m} \mathbf{d}_m|\phi_m\rangle\langle\phi_g| + \sum_{N} \mathbf{d}_N|\phi_N\rangle\langle\phi_g| + \text{H.c.} \tag{11}$$

It includes the transition dipole moments $\mathbf{d}_m$ of the various molecules. The $\mathbf{d}_N$ refer to the MNP.

E. Density Matrix Theory. Dissipative dynamics in the SC−MNP system are described in the framework of a density matrix theory. It accounts for plasmon decay and electron−vibrational coupling in the SC via respective dephasing rates. To stay simple, we focus on approximate density matrix equations where the dissipative part does not couple the time evolution of populations and coherences. To determine the absorption spectrum, off-diagonal density matrix elements of the type $\rho_{Ag}(t)$ (so-called coherences) are of particular interest (note that the quantum numbers A only cover excited electronic states). In the case of the site representation we identify the $|\phi_A\rangle$ with the states $|\phi_n\rangle$ and $|\phi_N\rangle$. The equations of motion for the coherences take the form

$$\frac{\partial}{\partial t}\rho_{ng}(t) = -i\tilde{\omega}_n\rho_{ng}(t) - \mathrm{i}\sum_{n'} j_{nn'}\rho_{n'g}(t) - \mathrm{i}\sum_{N} v_{nN}\rho_{Ng}(t) \tag{12}$$

and

$$\frac{\partial}{\partial t}\rho_{Ng}(t) = -\mathrm{i}\tilde{\omega}_N\rho_{Ng}(t) - \mathrm{i}\sum_{n} v_{Nn}\rho_{ng}(t) \tag{13}$$

Note the Introduction of $j_{nn'} = J_{nn'}/\hbar$, $v_{nN} = V_{nN}/\hbar$, $\tilde{\omega}_n = E_n/\hbar - \mathrm{i}\gamma_{\mathrm{Mol}}$, and $\tilde{\omega}_N = E_N/\hbar - \mathrm{i}\gamma_{\mathrm{pl}}$. The formulation of the density matrix theory using the exciton representation of the SC results in

$$\frac{\partial}{\partial t}\rho_{\alpha g}(t) = -\mathrm{i}\tilde{\omega}_\alpha\rho_{\alpha g}(t) - \mathrm{i}\sum_{N} v_{\alpha N}\rho_{Ng}(t) \tag{14}$$

and

$$\frac{\partial}{\partial t}\rho_{Ng}(t) = -\mathrm{i}\tilde{\omega}_N\rho_{Ng}(t) - \mathrm{i}\sum_{\alpha} v_{N\alpha}\rho_{\alpha g}(t) \tag{15}$$

We introduced $\tilde{\omega}_\alpha = E_\alpha/\hbar - \mathrm{i}\gamma_\alpha$ and $v_{\alpha N} = V_{\alpha N}/\hbar$. It is well-known how to calculate the exciton dephasing rates γ_α (see, for example, ref 2). Here, however, we consider them as new parameters.

III. ABSORPTION LINE SHAPE

The general form of the absorption line shape already introduced in eq 1 is given by

$$I(\omega) = Re\int_0^\infty \mathrm{d}t\ \mathrm{e}^{\mathrm{i}\omega t} C_{\mathrm{D-D}}(t) \tag{16}$$

It is expressed by the dipole−dipole correlation function. For the present application we can focus on its resonant part. We also state that for such small MNP as discussed here measured extinction spectra are dominated by radiation field absorption and not scattering. So the latter part will be neglected. Noting the system-reservoir description the correlation function takes the form (cf. Appendix C)

$$C_{\mathrm{D-D}}(t) = \mathrm{tr_S}\{\hat{\mu}[\mathcal{U}(t)\hat{\mu}|\phi_g\rangle\langle\phi_g|]\} \tag{17}$$

where $\mathcal{U}$ denotes the time evolution superoperator from which the density matrix equations introduced in section IIE result. The trace in eq 17 accounts for all electronic states included (they form the system S). The initially realized electronic ground state is characterized by $|\phi_g\rangle\langle\phi_g|$. $\hat{\mu}$ is the SC−MNP system dipole operator, written in a way to cover the case of equally and randomly oriented systems.

In the case of randomly oriented SC−MNP systems (the internal structures are identical for all members of the ensemble but the spatial orientation varies) the product of both $\hat{\mu}$ has to be understood as one-third of the scalar product of the vectorial dipole operators $\hat{\mu}\hat{\mu} = 1/3 \times [\hat{\boldsymbol{\mu}}\hat{\boldsymbol{\mu}}]$. If all SC−MNP systems are identical and have the same spatial orientation (this would be achievable on a surface and is typical for so-called meta materials), we have to set $\hat{\mu}\hat{\mu} = [\mathbf{n}\hat{\boldsymbol{\mu}}][\mathbf{n}\hat{\boldsymbol{\mu}}]$ where $\mathbf{n}$ is the polarization unit vector of the external field.

A. SC in the Site Representation. We describe the SC in the site representation and, first, focus on the case of randomly oriented SC−MNP systems. Therefore, the following quantity is defined

$$\hat{\boldsymbol{\sigma}}(t) = \mathcal{U}(t)\left(\sum_{n} \mathbf{d}_n|\phi_n\rangle\langle\phi_g| + \sum_{N'} d_{N'}|\phi_{N'}\rangle\langle\phi_g|\right) \tag{18}$$

The correlation function follows as

$$C_{\mathrm{D-D}}(t) = \frac{1}{3}\left(\sum_{n} [\mathbf{d}_n^{*}\boldsymbol{\sigma}_{ng}(t)] + \sum_{N} [\mathbf{d}_n^{*}\boldsymbol{\sigma}_{Ng}(t)]\right) \tag{19}$$

where we introduced the matrix elements $\boldsymbol{\sigma}_{ng}(t) = \langle\phi_n|\hat{\boldsymbol{\sigma}}(t)|\phi_g\rangle$, and $\boldsymbol{\sigma}_{Ng}(t) = \langle\phi_N|\hat{\boldsymbol{\sigma}}(t)|\phi_g\rangle$. We may deduce initial values as $\boldsymbol{\sigma}_{ng}(0) = \mathbf{d}_n$ and $\boldsymbol{\sigma}_{Ng}(0) = \mathbf{d}_N$. Next we introduce the Cartesian components $\sigma_{ng,j}(t) = [\mathbf{e}_j\boldsymbol{\sigma}_{ng}(t)]$ and $\sigma_{Ng,j}(t) = [\mathbf{e}_j\boldsymbol{\sigma}_{Ng}(t)]$. The absorption line shape, eq 16, follows as

$$I(\omega) = \frac{1}{3}Re\int_0^\infty \mathrm{d}t\ \mathrm{e}^{\mathrm{i}\omega t}\sum_{j}\left(\sum_{n} d_{nj}^{*}\sigma_{ng,j}(t) + \sum_{N} d_{Nj}^{*}\sigma_{Ng,j}(t)\right) \tag{20}$$

The $\sigma_{ng,j}(t)$ and $\sigma_{Ng,j}(t)$ obey eqs 12 and 13, respectively.

To consider the case of equally oriented SC−MNP systems, the correlation function is written as

$$C_{\mathrm{D-D}}(t) = \sum_{n} d_n^{*}s_{ng}(t) + \sum_{N} d_N^{*}s_{Ng}(t) \tag{21}$$

We used $d_n = [\mathbf{n}\mathbf{d}_n]$ and $d_N = [\mathbf{n}\mathbf{d}_N]$ and introduced

$$\hat{s}(t) = \mathcal{U}(t)\left(\sum_{n} d_n|\phi_n\rangle\langle\phi_g| + \sum_{N'} d_{N'}|\phi_{N'}\rangle\langle\phi_g|\right) = [\mathbf{n}\hat{\boldsymbol{\sigma}}(t)] \tag{22}$$

Note also $s_{ng}(0) = d_n$ and $s_{Ng}(0) = d_N$. The computation of respective matrix elements of $\hat{\boldsymbol{\sigma}}(t)$ has been already explained. Those are used to determine the absorption line shape in the case of equally oriented SC−MNP systems as

dx.doi.org/10.1021/jp305505c | J. Phys. Chem. A 2012, 116, 11330−11340

$$I(\omega) = Re \int_0^\infty \mathrm{d}t\ \mathrm{e}^{\mathrm{i}\omega t}\Big(\sum_n d_n^* \sum_j n_j \sigma_{mg,j}(t) + \sum_N d_N^* \sum_j n_j \sigma_{Ng,j}(t)\Big) \tag{23}$$

B. SC in the Exciton Representation. If the SC is described in the exciton representation as given in eq 9, there remains the exciton−MNP coupling, which can be accounted for analytically when the absorption line shape is computed. Although such an independent computation is not necessary, the approximate expression (it neglects particular self-energy contributions) is of some interest. It takes the impressive form (for details see Appendix D):

$$I(\omega) = -\mathrm{Im} \sum_\alpha \frac{D_\alpha^{(+)}(\omega)\, D_\alpha(\omega)}{\omega - \tilde{\omega}_\alpha - \Sigma_{\alpha\alpha}(\omega)} - \mathrm{Im} \sum_N \frac{|d_N|^2}{\omega - \tilde{\omega}_N} \tag{24}$$

The absorption line shape is given by changed contributions due to the various exciton levels and by the unchanged absorption of the MNP. The changed SC exciton contributions include renormalized dipole moments

$$D_\alpha(\omega) = d_\alpha + \sum_N \frac{d_N v_{N\alpha}}{\omega - \tilde{\omega}_N} \tag{25}$$

where $D_\alpha^{(+)}$ is obtained from D_α by replacing d_α and d_N by d_α^* and d_N^*, respectively. Moreover, the exciton energies are shifted and additionally broadened. $\Sigma_{\alpha\alpha}(\omega)$ denotes the diagonal part of the self-energy, eq D7, due to excitation energy exchange between the particular exciton level and the MNP. We will use eq 24 later on to interpret the line shape computed in the site representation.

IV. ABSORPTION SPECTRA OF A SC ATTACHED TO A SPHERICAL MNP

Next we specify the formulas presented so far to a spherical MNP. In such a case multipole excitations are the most prominent excitations of the electron system. We may introduce the multipolar indices l and m and write for the MNP Hamiltonian, eq 3:

$$H_{\mathrm{pl}} = \sum_{l,m} E_{lm} |\psi_{lm}\rangle\langle\psi_{lm}| \tag{26}$$

Table 1. Used Parameters for the SC and a Spherical Gold MNP (Explanation in Text)

N_{Mol}	10
E_{Mol}	varied around E_{pl}
d_{Mol}	8 D
Δx_{Mol}	1.2 nm
γ_{Mol}	3 meV
a	10 nm
$E_{l=1}$	2.60 eV
$E_{l=2}$	2.86 eV
$E_{l=3}$	2.96 eV
$E_{l=4}$	3.02 eV
d_{pl}	2925 D
γ_{pl}	28.6 meV

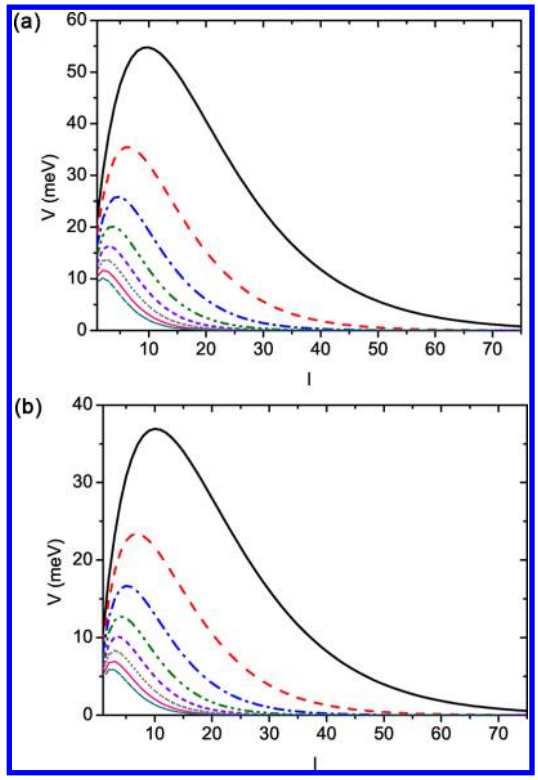

Figure 3. Reduced coupling matrix elements $V(nl)$ between molecule n and the MNP, eq 28, versus the multipole index l and for different molecule MNP surface distances ΔX (the large numbers of l motivate for a continuous line presentation). ΔX varies between 1 and 4.5 nm in steps of 0.5 nm. Upper panel: $\mathbf{d}_{\mathrm{Mol}}$ parallel to the vector $\mathbf{X}$ connecting the molecule and the MNP center of mass ($\mathbf{d}_{\mathrm{Mol}} \parallel \mathbf{e}_x$, J-aggregate configuration), lower panel: $\mathbf{d}_{\mathrm{Mol}}$ perpendicular to $\mathbf{X}$ ($\mathbf{d}_{\mathrm{Mol}} \parallel \mathbf{e}_y$, H-aggregate configuration). Lines: solid black line, ΔX = 1 nm; dashed red line, ΔX = 1.5 nm; dashed dotted blue line, ΔX = 2 nm; dashed dotted green line, ΔX = 2.5 nm; short dashed violet line, ΔX = 3 nm; short dotted gray line ΔX = 3.5 nm; thin solid pink line, ΔX = 4 nm; thin dashed dark cyan line, Δx = 4.5 nm.

Note that the multipolar indices l = 0, 1, 2, ... and $m = -l, ..., l$ characterize the collective MNP state and not that of a single electron. Some similarities of the E_{lm} with the Mie frequencies

$$\omega_l^{(M)} = \sqrt{l/(2l+1)}\,\omega_{\mathrm{pl}} \tag{27}$$

have to be expected at large sphere diameters[25] (the bulk plasma frequency is $\omega_{\mathrm{pl}}^2 = 4\pi n_{\mathrm{el}} e^2/m_{\mathrm{el}}$).

The expression eq 26 shall be understood as a part of a system-reservoir description. It is extended in the density matrix description of section IIE by the introduction of dephasing rates γ_{pl} reflecting the short plasmon lifetime. The latter quantity has been determined in refs 26−28 for dipole plasmons. Focusing on a Au MNP with a 20 nm diameter we use γ_{pl} according to Table 1. Its choice for higher multipole excitations is not yet clear and will be considered as a parameter to be varied in the following computations. Concerning the MNP excitation energies E_{lm}, that one for the dipole plasmon is known from experiment (cf. Table 1 and ref 28). We use this measured value to compute higher excitation energies according to the Mie formula as $E_l = (3l/(2l+1))^{1/2} E_{l=1}$. The overestimation of the dipole-plasmon resonance by the Mie frequencies, eq 27, could be related to the effect of spill-out electrons and a coupling to individual electron−hole pair excitations.[28]

dx.doi.org/10.1021/jp305505c | J. Phys. Chem. A 2012, 116, 11330−11340

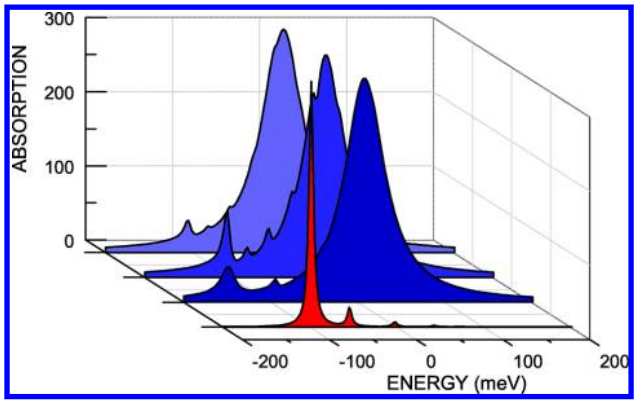

Figure 4. SC−MNP absorption line shape $I(\omega)/N_{\mathrm{Mol}}d_{\mathrm{Mol}}{}^2$ versus $\hbar\omega - E_{l=1}$ (case $E_{\mathrm{Mol}} = E_{l=1}$). The MNP is placed at the right end of the SC and the MNP center of mass is located at the x-axis defined by the chain of molecules taken in J-aggregate configuration (molecular transition dipole moments point in the x-direction). The distance ΔX between the last molecule of the SC and the MNP surface is varied. Background to foreground curves: ΔX = 2.5 nm and random oriented SC−MNP complexes (l_{max} = 25), ΔX = 2.5 nm and equally oriented SC−MNP complexes ($\mathbf{n} \parallel \mathbf{d}_{\mathrm{Mol}}$, l_{max} = 25), ΔX = 1 nm and equally oriented SC−MNP complexes ($\mathbf{n} \parallel \mathbf{d}_{\mathrm{Mol}}$, l_{max} = 65). The foremost red filled curve shows the SC absorption line shape in the absence of the MNP (increased by about 5×10^3).

To model Frenkel excitons in a SC, we consider a chain of 10 identical molecules. All SC parameters will be varied to cover different examples (the excitation energy E_{mol} of the individual molecules is moved through the dipole plasmon resonance of the MNP). As an upper limit we quote in Table 1 values for the intermolecular distance of 1.2 nm and for the transition dipole moment of 8 D. The chosen values result in a rather large nearest-neighbor excitonic coupling. $J_{nn\pm1}$ amounts −46 meV in a J-aggregate configuration (transition dipole moments parallel to the chain) and 23 meV in a H-aggregate configuration (transition dipole moments perpendicular to the chain). The dipole−dipole coupling model introduced for this computation can be justified by the used intermolecular distance. Because the excitation spectra are dominated by exciton levels, we neglect any direct coupling to vibrational modes (the coupling is only considered by the dephasing rate γ_{Mol} as given in Table 1).

The necessary specification of the molecule−MNP coupling, eq 4, to a spherical MNP has been detailed in Appendix B. The involved matrix elements $V_{n,lm}$ of energy exchange between a MNP plasmon excitation and the molecule n is given in eq B4. It includes the de-excitation of a multipole plasmon in the MNP with multipole moment $e\mathcal{Q}_{lm}$. Following ref 29 we estimate $e\mathcal{Q}_{lm}$ in the framework of the plasmon resonance approximation as $\hbar\omega_i^{(\mathrm{M})}(a^{2l+1}/2E_l)^{1/2}$ (cf. Appendix A1, a is the MNP radius). As indicated above, the energies E_l entering the plasmon Hamiltonian may deviate from $\hbar\omega_i^{(\mathrm{M})}$. And, the expression for $e\mathcal{Q}_{lm}$ is based on a constant ground-state MNP electron density $n_0(\mathbf{x})$ across the MNP. Because this assumption ignores spill−out electrons, one may replace E_{lm} by the Mie frequencies $\omega_i^{(\mathrm{M})}$. This, however, underestimate $e\mathcal{Q}_{lm}$ somewhat (see below).

Optical absorption of a weak external radiation field mainly results in dipole−plasmon formation. Accordingly, the general MNP transition dipole moment $\mathbf{d}_{\mathrm{N}}$ introduced in eq 11 and specified to a spherical MNP reduces to $\mathbf{d}_{lm} = \delta_{l,1}\mathbf{d}_{1m}$. The Cartesian components are $\mathbf{d}_{1m=0} = \mathbf{e}_z d_{\mathrm{pl}}$ and $\mathbf{d}_{1m=\pm1} = (\mp\mathbf{e}_x + i\mathbf{e}_y)d_{\mathrm{pl}}/\sqrt{2}$, where we also introduced $d_{\mathrm{pl}} = \hbar\omega_{l=1}^{(\mathrm{M})}(a^3/2E_{l=1})^{1/2}$ (cf. also Table 1).

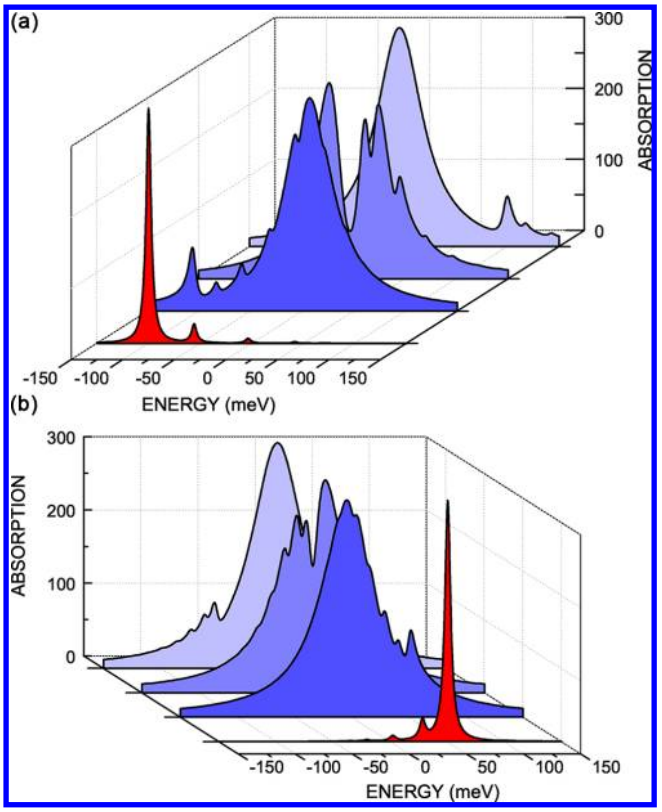

Figure 5. SC−MNP absorption line shape $I(\omega)/N_{\mathrm{Mol}}d_{\mathrm{Mol}}{}^2$ versus $\hbar\omega - E_{l=1}$ for equally oriented SC−MNP complexes ($\mathbf{n} \parallel \mathbf{d}_{\mathrm{mol}}$) and a variation of the molecular excitation energy E_{mol} (same geometry as in Figure 4, ΔX = 2.5 nm). Upper panel: SC in J-aggregate configuration (molecular transition dipole moments point in the x-direction). Background to foreground curves: $E_{\mathrm{Mol}} = E_{l=1}$ + 200 meV, $E_{\mathrm{Mol}} = E_{l=1}$ + 100 meV, $E_{\mathrm{Mol}} = E_{l=1}$. Lower panel: SC in H-aggregate configuration (molecular transition dipole moments point in y-direction). Background to foreground curves: $E_{\mathrm{Mol}} = E_{l=1}$−100 meV, $E_{\mathrm{Mol}} = E_{l=1}$ − 50 meV, $E_{\mathrm{Mol}} = E_{l=1}$. The foremost red filled curves show the SC absorption line shape in the absence of the MNP (increased by about 5×10^3, at $E_{\mathrm{Mol}} = E_{l=1}$).

A. Reduced Molecule MNP Coupling Matrix Elements.

To characterize the coupling strength between the molecular transition dipole moment and the MNP transition multipole moments, we proceed as follows. Provided that the $V_{n,lm}$ are weak enough, the molecule−MNP coupling can be described by a Förster-like transition rate. It would be determined by the square of $V_{n,lm}$, by the energy conserving δ−function, and by a summation with respect to the multipole indices (cf., e.g., ref 2). Because the MNP energies are independent of m, we arrive at the square of a reduced coupling matrix element

$$V^2(n,l)(\mathbf{X}_n) = \sum_m |V(n,lm)|^2 \tag{28}$$

which depends on the position $\mathbf{X}_n$ of molecule n relative to the MNP's center of mass.

Figure 3 displays $V(n,l)(\mathbf{X}_n)$ versus l for different molecule MNP geometries. In the case $\mathbf{d}_{\mathrm{Mol}} \parallel \mathbf{X}_n$ (J-aggregate configuration of the SC) as well as in the case $\mathbf{d}_{\mathrm{Mol}} \perp \mathbf{X}_n$ (H-aggregate configuration of the SC) the different curves look similar. A detailed inspection of eq B4 shows that the two types of $V(n,l)(\mathbf{X}_n)$ are characterized by similar expressions.

dx.doi.org/10.1021/jp305505c | J. Phys. Chem. A 2012, 116, 11330−11340

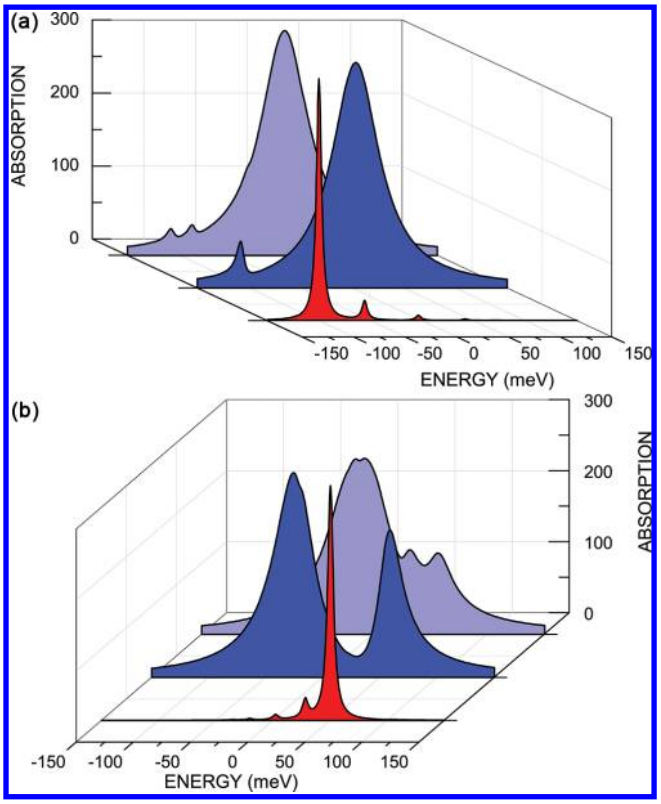

Figure 6. SC−MNP absorption line shape $I(\omega)/N_{\mathrm{Mol}}d_{\mathrm{Mol}}{}^2$ versus $\hbar\omega - E_{l=1}$ and at $E_{\mathrm{Mol}} = E_{l=1}$ ($\mathbf{n} \parallel \mathbf{d}_{\mathrm{Mol}}$). The MNP is placed in front of the chain center, but with its surface 2.5 nm apart in the *y*-direction. Upper panel: J-aggregate configuration (molecular transition dipole moments point in the *x*-direction). Lower panel: H-aggregate configuration (molecular transition dipole moments point in *y*-direction). Middle curves: case of equally oriented SC−MNP complexes. Background curves: case of random oriented of SC−MNP complexes complex. The foremost red filled curves show the SC absorption line shape in the absence of the MNP (increased by about 5×10^3).

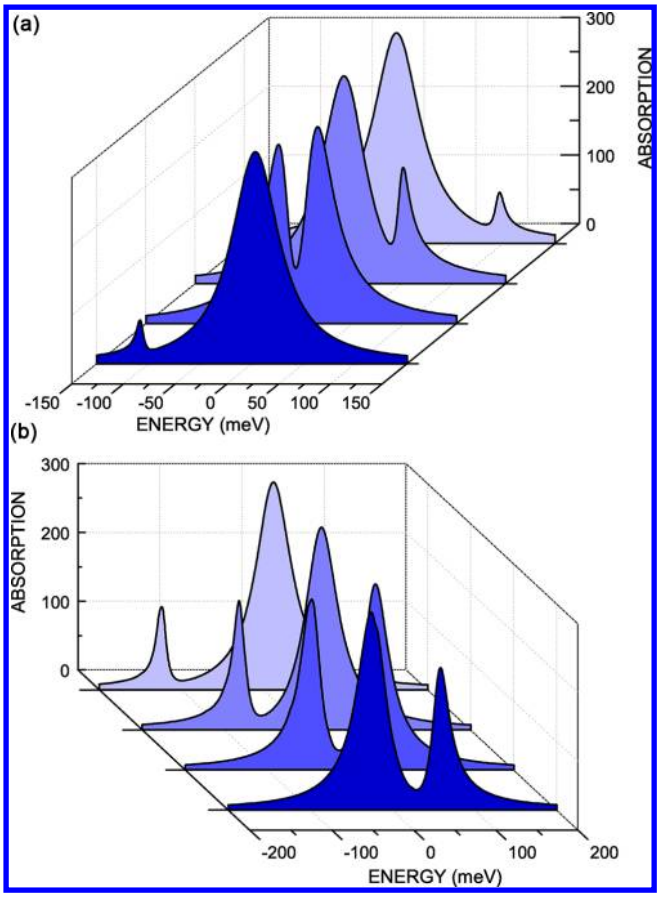

Figure 7. SC−MNP absorption line shape $I(\omega)/N_{\mathrm{Mol}}d_{\mathrm{Mol}}{}^2$ versus $\hbar\omega - E_{l=1}$ for the same geometry as used in Figure 6 and for the case of equally oriented SC−MNP complexes. Variation of E_{Mol}. Upper panel: J-aggregate configuration, background to foreground curves: $E_{\mathrm{Mol}} = E_{l=1} + 200$ meV, $E_{l=1}+150$ meV, $E_{l=1} + 100$ meV, $E_{l=1}$. Lower panel: H-aggregate configuration, background to foreground curves: $E_{\mathrm{Mol}} = E_{l=1} - 150$ meV, $E_{l=1} - 100$ meV, $E_{l=1} - 50$ meV, $E_{l=1}$.

Interestingly, $V(n,l)(\mathbf{X}_n)$ increases with increasing l up to a maximum. In the case of the smallest molecule MNP surface distance ($\Delta X = 1$ nm) the maximum value is more than 2 times larger than the coupling of the molecule to dipole plasmon excitations of the MNP. Of course, this behavior is connected with the increasing number of m if l is increased. A further increase of l results in decreasing coupling matrix elements. The maximum of $V(n,l)(\mathbf{X}_n)$ is moved to smaller l if $\mathbf{X}_n$ is increased.

Translated to the coupling of the MNP to the complete SC, only those molecules are affected by higher multipolar excitations which are close enough to the MNP surface. At a geometry shown in Figure 1 (the SC and the MNP form a common chain) and at a distance $\Delta X = 1$ nm between the last molecule of the SC and the MNP surface, the last but one molecule is 2.2 nm apart from the MNP surface and its coupling to the MNP excitations is characterized by something between the blue and the green curves of the two panels in Figure 3. Now, the coupling to dipole plasmons is only slightly smaller than the maximum of the curves (at $l = 4$). All other molecules of the SC are characterized by coupling strengths much weaker than the foregoing ones. They are also dominated by the coupling to the dipole plasmon.

In the spectral computations we will also choose $\Delta X = 2.5$ nm as the distance between the last molecule of the SC and the MNP surface. Then, the coupling to the last but one molecule in the SC is given by a curve between the gray and the pink lines (maximum at $l = 3$). This observation is valid for a J- as well as a H-aggregate configuration of the SC.

B. Absorption Line Shapes. The absorption spectra are displayed as $I(\omega)/N_{\mathrm{Mol}}d_{\mathrm{Mol}}{}^2$ (getting in this way the dimension of time, picoseconds in the respective figures). Figure 4 shows some first examples for a SC−MNP configuration as presented in Figure 1 (the MNP is placed at the right end of the SC and the MNP center of mass is located at the *x*-axis defined by the chain of molecules taken in J-aggregate configuration, i.e., molecular transition dipole moments point in the *x*-direction). For comparison, the line shape of the isolated SC (absence of the MNP) has been also drawn. In absolute values this absorption is about 5000 times smaller than the one of the SC−MNP complex. Figure 4 includes the case of equally and of randomly oriented SC−MNP complexes. Moreover, the two distances $\Delta X = 1$ and 2.5 nm between the last molecule of the SC and the MNP surface are considered. Note that the computations for the case $\Delta X = 1$ nm require the consideration of multipole indices up to $l = 65$ whereas in the case $\Delta X = 2.5$ nm values of $l = 25$ are sufficient to achieve convergence.

Of most interest is the curve following for equally oriented SC−MNP complexes and $\Delta X = 2.5$ nm. Here, the low energy shoulder of the broad MNP absorption includes various peaks that refer to the different exciton levels of the SC (cf. also

dx.doi.org/10.1021/jp305505c | J. Phys. Chem. A 2012, 116, 11330−11340

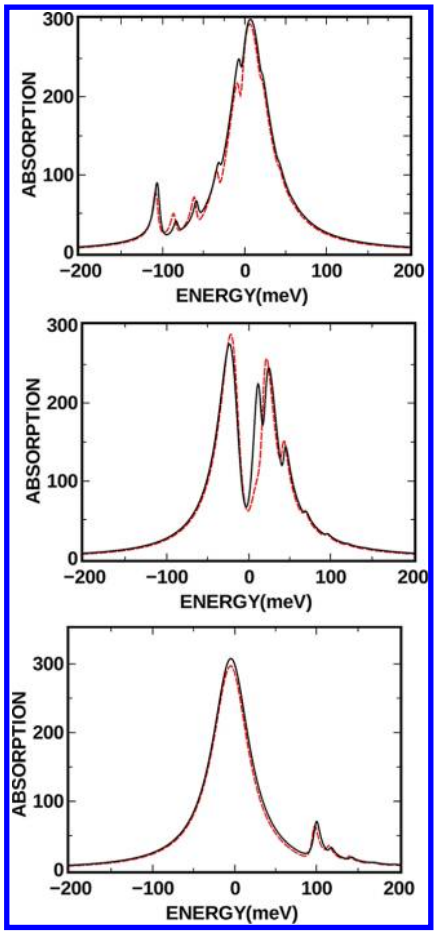

Figure 8. SC−MNP absorption line shape $I(\omega)/N_{\mathrm{Mol}}d_{\mathrm{Mol}}^2$ versus $\hbar\omega - E_{l=1}$ computed with the exact expression, eq 23 (solid black lines), and the approximate expression, eq 24, formulated in the SC−exciton representation (dashed red lines). The same configuration as used in the upper panel of Figure 5 has been taken (SC in J-aggregate configuration, case of equally oriented SC−MNP complexes). Upper panel: $E_{\mathrm{Mol}} = E_{l=1}$. Middle panel: $E_{\mathrm{Mol}} = E_{l=1} + 100$ meV. Lower panel: $E_{\mathrm{Mol}} = E_{l=1} + 200$ meV.

Figure 2). This is in strong contrast to the line shape of the isolated SC where the lowest exciton level dominates. Thus, an oscillator redistribution relative to the lowest exciton level appears when the SC is coupled to a MNP (cf. also the discussion in the subsequent section IVC). This observation has been already reported by us recently in ref 22 but restricting the MNP description to their dipole plasmon excitations only.

The present computations confirm the former results by accounting for all multipole excitations. Those are included via the SC−MNP coupling matrix elements, eq B4. What happens can be somewhat visualized in using the energy level scheme (in the SC exciton representation) of Figure 2. The higher multipole excitations are not involved in MNP optical absorption but they contribute to the SC−MNP coupling. According to eq 14 exciton coherences $\rho_{\alpha g}$ are transferred into the various MNP coherences ρ_{Ng} ($N = lm$) determined by eq 15 and vice versa. If there is an efficient net redistribution of magnitude from the $\rho_{\alpha g}$ to the ρ_{Ng}, the exciton levels may contribute less to the absorption. This effect can be seen if one compares the case discussed so far ($\Delta X = 2.5$ nm) with the case of $\Delta X = 1$ nm. Because the SC−MNP coupling is stronger for a smaller relative SC−MNP distance (cf. Figure 3), the respective absorption shown in Figure 4 only displays two exciton peaks. They become also less visible when changing to the case of randomly oriented SC−MNP complexes.

As already indicated at the beginning of section IV, the choice of the multipole state lifetimes is not clear. We tested different cases including a doubling of the broadening of higher multipole excitations compared to the dipole excitation and the case where the broadening increases as $l\gamma_{\mathrm{pl}}$ (with the dipole plasmon broadening γ_{pl} according to Table 1). All examples indicated less influence except the broadening is increased by 2 or 3 orders of magnitude compared to γ_{pl} (now, higher multipole states decay instantenously and do not contribute). So, all calculations have be done in taking $2\gamma_{\mathrm{pl}}$ for the broadening of higher multipole levels.

The SC−MNP geometry displaying all exciton levels as shown in Figure 4 is further analyzed in Figure 5. We took the SC in J- and H-aggregate configuration and moved the molecular excitation energy E_{Mol} through the dipole plasmon resonance $E_{l=1}$. As already shown in Figure 4, a MNP induced oscillator strength redistribution remains visible with the strongest effect if the dominant exciton level (lowest one for the J-aggregate configuration and highest one for the H-aggregate configuration) comes into resonance to the dipole plasmon of the MNP.

The absorption line shape becomes less rich if we change the SC−MNP geometry to the case considered in Figure 6. Now, the MNP is positioned in front of the SC (at the center of the SC but with the distance ΔX between the chain and the MNP surface in y-direction). The variation of molecular excitation energy E_{mol} with respect to the dipole plasmon resonance $E_{l=1}$ for the same geometry is shown in Figure 7. Here, a pronounced splitting of the dominant exciton level (the one with the largest oscillator strength in the isolated SC) and the MNP dipole resonance becomes visible.

C. Absorption Line Shapes Using the Exciton Representation for the SC. There is no need to again calculate the absorption line shape using the exciton representation of the SC. We only present some data here to check the validity of the approximate expression, eq 24, which offers a nice and simple explanation of the line shape.

Figure 8 shows the absorption line shapes for a configuration already used in the upper panel of Figure 5 (J-aggregate configuration, case of equally oriented SC−MNP complexes). The agreement with the exact results (in the sense of a use of eq 23) is nice as long as exciton levels are concerned which are about 100 meV apart from the dipole plasmon resonance $E_{l=1}$. If not, the approximate formula eq 24, which ignores off-diagonal contributions of the exciton self-energy, eq D7, results in a 10−20 meV red shift of the exciton peaks. This shift is much larger than the one appearing in the exact computation (3−5 meV). So, we can conclude that the main effect of the MNP on the SC absorption in the coupled SC−MNP complex is a strong increase of the exciton oscillator strength. The exciton resonances appear in the broad background of the MNP absorption. In the present J-aggregate configuration higher lying exciton levels get much more oscillator strength relative to the lowest exciton level compared to the case of the isolated SC.

V. CONCLUSIONS

A theoretical analysis of the absorption line shape of a supramolecular complex (SC) placed in the proximity of a spherical metal nanoparticle (MNP) was offered. The computations have been based on a density matrix description

dx.doi.org/10.1021/jp305505c | J. Phys. Chem. A 2012, 116, 11330−11340

of the absorption and accounted for all multipole excitations of the MNP. The microscopic description of the SC−MNP complex includes the mutual Coulomb interaction dominated by an energy exchange coupling between the SC and the MNP with its multipolar excitations. An oscillator strength redistribution relative to the lowest exciton level appears for particular geometries of the SC−MNP complex. This result, already reported by us in ref 22 by restricting the MNP description to their dipole plasmon excitations only, survives the more correct description including MNP multipole excitations.

Of course this is a subtle effect that requires the absence of disorder in the ensemble of SC−MNP complexes. If the exciton parameters and the SC−MNP coupling fluctuate somewhat, the presence of various SC exciton levels is washed out (an effect which might be responsible for the observation of a single exciton peak only in refs 9−11).

It is of particular interest to extend the present studies to more complex arrangements with two or three MNP of different geometry and with SC forming, for example, 2d structures. Respective computations are under work.

APPENDIX A: COLLECTIVE EXCITATIONS OF A MNP

In the present section we motivate the introduction of a plasmon Hamiltonian like the one given in eq 2 and specify it to a spherical MNP. It is the weakness of the subsequent derivation of H_{pl} that the Hamiltonian does not follow directly by a sequence of approximations from H_{MNP}, eq 3. Instead, the treatment advocated in refs 25 and 30−33 is based on the introduction of an effective Hamiltonian and the analysis of particular MNP energy moments. According to ref 31 collective excited states and energies of the MNP electron system are determined by using the ansatz $\psi(x) = \exp(i\hat{Q})\psi_0(x)$ for the excited-state wave function (x abbreviates the whole set of MNP electron coordinates). Accordingly, the excited state is obtained from the ground state by a deformation due to the operator $\hat{Q}$. The latter should be of the form $\hat{Q} = \sum_j q(\mathbf{x}_j)$; i.e., it is a sum of single electron operators that only depend on the electron coordinates. Considering the case of a spherical MNP the idea of this ansatz is to mimic multipole excitations of the MNP electron system. Therefore, the various $q(\mathbf{x})$ are identified with multipole operators

$$q_{lm}(\mathbf{x}) = \sqrt{4\pi/(2l+1)}\, x^l Y_{lm}(\vartheta,\varphi) \tag{A1}$$

The x, ϑ, and φ are the spherical coordinates of $\mathbf{x}$, and the $Y_{lm}(\vartheta,\varphi)$ denote spherical harmonics. Because an ansatz is used for the electronic wave function, we can only expect to get that part of the energy spectrum which is compatible with the wave function ansatz.

To demonstrate that the $\psi(x) = \exp(i\hat{Q})\psi_0(x)$ represent good approximations of the collective-state eigenfunctions of H_{MNP} and to show how to get the related approximations for the eigenenergies, a time-dependent variant of $\psi(x)$ is introduced. It takes the form $\psi(x;\, \alpha(t),\, \beta(t)) = \exp(i\alpha(t)\hat{Q})\exp(im_{el}\beta(t)[H_{MNP},\hat{Q}]_-)\psi_0(x)$.[31] Equations of motion for the time-dependent functions $\alpha(t)$ and $\beta(t)$ are obtained from a variational principle (which is equivalent to the time-dependent Schrödinger equation). These equations of motion can be interpreted as a Lagrangian formulation of the dynamics with generalized coordinates and velocities. Then, one changes to canonical equations with canonical variables defining a Hamilton function. A particular choice of the canonical variables[31] results in a Hamilton function, which is understood to reproduce in a good approximation those eigenvalues of H_{MNP} that correspond to collective excitations generated by the operator $\hat{Q}$. Introducing a harmonic approximation of the respective potential energy an oscillator frequency ω can be directly deduced and is identified with the approximate eigenvalues of H_{MNP}, eq 3. According to the specific ansatz for the time-dependent MNP electron wave function the oscillator frequencies ω appear as a ratio of energy moments, i.e., we get $\omega^2 = m_3/m_1$. The energy moments m_1 and m_3 are specific cases of the general type

$$m_n(\hat{Q}) = \sum_k (E_k)^n |\langle\psi_k|\hat{Q}|\psi_0\rangle|^2 \tag{A2}$$

where the E_k and ψ_k have been already introduced as eigenvalues and eigenstates of the MNP electron system, respectively (note that the definition provides $E_0 = 0$). The possibility to compute the spectrum of H_{MNP} by the moments m_1 and m_3 is based on the observation that they are identical with particular ground-state expectation values. For example, the use of some simple algebra demonstrates that

$$m_1(\hat{Q}) = \langle\psi_0|\hat{Q}H_{MNP}\hat{Q}|\psi_0\rangle \equiv \frac{1}{2}\langle\psi_0|[\hat{Q},[H_{MNP},\hat{Q}]_-]_-|\psi_0\rangle \tag{A3}$$

provided $\hat{Q}$ is Hermitian. Such a relation has been used, for example, in ref 25 to compute multipole electron density vibrations of alkali clusters. And, the recovery of the Mie frequencies in large diameter clusters could be demonstrated.

If the operator $\hat{Q}$ is not Hermitian, we have to distinguish between $m_1(\hat{Q}) = \langle\psi_0|\hat{Q}^+H_{MNP}\hat{Q}|\psi_0\rangle$ and $m_1(\hat{Q}^+) = \langle\psi_0|\hat{Q}H_{MNP}\hat{Q}^+|\psi_0\rangle$. We note that $[H_{MNP},\hat{Q}]_-$ coincides with a commutator including the kinetic energy only and derive

$$\begin{aligned} &m_1(\hat{Q}) + m_1(\hat{Q}^+) \\ &\quad = \langle\psi_0|[\hat{Q}^+,[H_{MNP},\hat{Q}]_-]_-|\psi_0\rangle \\ &\quad = \frac{\hbar^2}{m_{el}}\int d^3\mathbf{x}\ |\nabla q(\mathbf{x})|^2 n_0(\mathbf{x}) \end{aligned} \tag{A4}$$

Here, we introduced the single electron operator $q(\mathbf{x})$ and the single electron density of the MNP electronic ground state $n_0(\mathbf{x}) = N_{el}\int dx\ \delta(\mathbf{x}-\mathbf{x}_1)\ |\psi_0(x)|^2$. Higher moments cannot be expressed by the single electron density in this simple way. Different types of approximations, for example, in the framework of DFT are necessary (for more details on this item and the distinction between surface and volume plasmons we refer to ref 25). Because $m_1(\hat{Q}^+) = (m_1(\hat{Q}))^*$ and both moments are real, we get $m_1(\hat{Q}) = m_1(\hat{Q}^+)$.

1. Plasmon Resonance Approximation

A single matrix element of the type $\langle\psi_\kappa|\hat{Q}|\psi_0\rangle$ can be obtained from the first moment m_1 if the so-called *plasmon resonance approximation* is carried out.[29] To motivate this approximation, we assume that $\hat{Q}$ generates a state $\hat{Q}\psi_0$ that approximates a possible collective excitation of the MNP electron system with state vector ψ_κ rather well. Accordingly, we may set

$$m_1(\hat{Q}) \approx E_\kappa |\langle\psi_\kappa|\hat{Q}|\psi_0\rangle|^2 \tag{A5}$$

The summation with respect to the whole set of MNP eigenstates has been reduced to a single (resonant) state ψ_κ. Noting eq A4 and $m_1(\hat{Q}) = m_1(\hat{Q}^+)$ the transition matrix element is determined by a single electron integral including

the single electron quantity $q(x)$ and the MNP ground-state electron density. If E_κ and n_0 are independently known, the transition matrix element can be computed (except an unknown phase factor).

Next, the plasmon resonance approximation is specified to multipole excitations of a spherical MNP. Accordingly, we choose for $q(\mathbf{x})$ the multipole operator q_{lm}, eq A1, with a particular choice of the multipolar indices l and m. The plasmon resonance approximation reads

$$m_1(\hat{Q}_{lm}) \approx E_{lm}\,|\langle\psi_{lm}|\hat{Q}_{lm}|\psi_0\rangle|^2 \tag{A6}$$

The expression states that the multipole deformation of the MNP electronic ground state $Q_{lm}\psi_0(r)$ is nearly identical with a respective multipole excitation of the electron system with energy E_{lm} and with wave function ψ_{lm}. So, we arrive at

$$\frac{\hbar^2}{m_{\mathrm{el}}}\int \mathrm{d}^3\mathbf{x}\;|\nabla q_{lm}|^2 n_0(\mathbf{x}) \approx 2E_{lm}\,|\langle\psi_{lm}|\hat{Q}_{lm}|\psi_0\rangle|^2 \tag{A7}$$

For a constant density in the MNP the single electron integral is easily computed,[29] and the left-hand side of eq A7 takes the form $(\hbar\omega_l^{(\mathrm{M})})^2 a^{2l+1}/e^2$ ($\omega_l^{(\mathrm{M})}$ is the Mie frequency, eq 27 and a denotes the radius of the MNP).

APPENDIX B: COUPLING OF A MOLECULE TO A SPHERICAL MNP

In the case of a spherical MNP we expect excited electronic states ψ_{lm} of multipolar type (cf. eq A6). To account for these excitations when determining the SC−MNP coupling, we start from the energy exchange coupling, eq 6, where the molecule is represented by its transition dipole moment only. If one carries out a multipole expansion of the MNP transition density in the electric-field expression, eq 7, one gets

$$\mathbf{E}_{k0}(\mathbf{X}) = -\nabla_{\mathbf{X}}\sum_{l,m}\sqrt{\frac{4\pi}{2l+1}}\,\frac{eQ^*_{lm}(k0)\,Y_{lm}(\vartheta,\varphi)}{X^{l+1}} \tag{B1}$$

with the MNP transition multipole moments

$$Q_{lm}(k0) = \int \mathrm{d}^3\mathbf{x}\; q_{lm} n_{k0}(\mathbf{x}) = \langle\psi_k|\hat{Q}_{lm}|\psi_0\rangle \tag{B2}$$

The multipole moment operators q_{lm} have been defined in eq A1. The matrix element with $\hat{Q}_{lm}$ is the many-electron variant of the foregoing single coordinate expression.

Remembering the plasmon resonance approximation, eqs A6, we consider $Q_{lm}(k0)$ to be nonzero only, if the quantum number k corresponds to a collective state ψ_{lm} with multipolarity according to l and m. So we get $Q_{lm}(k0) \approx \delta_{k,lm}\langle\psi_{lm}|\hat{Q}_{lm}|\psi_0\rangle$. The right-hand side of this expression, however, is independently known from eq A7 (except a phase factor).

According to this reasoning the SC−MNP coupling in eq 8 reads

$$H_{\text{SC-MNP}} = \sum_{n,ml}(V_{n,ml}|\phi_n\rangle\langle\phi_{ml}| + \text{H.c.}) \tag{B3}$$

and is determined by the matrix elements

$$V_{n,lm} = \sqrt{\frac{4\pi}{2l+1}}\,eQ^*_{lm}[\mathbf{d}_n\nabla_{\mathbf{X}}]\frac{Y_{lm}(\vartheta,\varphi)}{X^{l+1}} \tag{B4}$$

with $Q_{lm} = \langle\psi_{lm}|\hat{Q}_{lm}|\psi_0\rangle$ (the spherical coordinates belong to molecule n what has not been indicated separately).

Finally, we shortly comment on a computation of $\nabla_{\mathbf{X}}Y_{lm}(\vartheta,\varphi)/X^{l+1}$. Therefore, $\nabla_{\mathbf{X}}$ is used in spherical coordinates according to $\mathbf{e}_X\partial/\partial X + \mathbf{e}_\varphi/X\sin\vartheta\times\partial/\partial\varphi + \mathbf{e}_\vartheta/X\times\partial/\partial\vartheta$. The derivatives with respect to X and to φ are trivial. However, the derivative with respect to ϑ requires some more effort. Noting the recursion relation for the associated Legendre polynomials $\partial P_l^m(x)/\partial x = -mxP_l^m(x)/(1-x^2) - P_l^{m+1}(x)/(1-x^2)^{1/2}$ one arrives at

$$\nabla_{\mathbf{X}}\frac{Y_{lm}(\vartheta,\varphi)}{X^{l+1}} = \frac{1}{X^{l+2}}\Bigg(-\mathbf{e}_X(l+1)Y_{lm}(\vartheta,\varphi) + \mathrm{i}\mathbf{e}_\varphi\frac{mY_{lm}(\vartheta,\varphi)}{\sin\vartheta} + \mathbf{e}_\vartheta(m\cot\vartheta Y_{lm}(\vartheta,\varphi) + \mathrm{e}^{-\mathrm{i}\varphi}\sqrt{(l-m)(l+m+1)}\,Y_{lm+1}(\vartheta,\varphi))\Bigg) \tag{B5}$$

APPENDIX C: DIPOLE−DIPOLE CORRELATION FUNCTION AND DENSITY OPERATOR PROPAGATION

To get the linear susceptibility defining the absorption coefficient, one has to linearize the dipole operator expectation value $\mathrm{tr}_S\{\hat{\rho}(t)\hat{\boldsymbol{\mu}}\}$ with respect to the exciting field $\mathbf{E}$. Therefore, the reduced density operator $\hat{\rho}(t)$ is determined linearly in $\mathbf{E}$ (the expression indicates that $\hat{\mu}$ is exclusively defined with respect to the primary system S).[2,3] A standard treatment gives (permanent dipole moments do not exist)

$$\hat{\rho}^{(1)}(t) = \frac{\mathrm{i}}{\hbar}\int_{t_0}^{t}\mathrm{d}\tau\;\mathcal{U}(t-\tau)\,\mathbf{E}(\tau)[\hat{\mu},\mathcal{U}(\tau-t_0)\hat{\rho}_{\mathrm{eq}}]_- \tag{C1}$$

where $\mathcal{U}$ is the time evolution superoperator at the absence of the field and $\hat{\rho}_{\mathrm{eq}}$ the initial equilibrium value of the reduced density operator. We note for the polarization (n is the volume density of the SC−MNP systems, $t_0\to\infty$)

$$\mathbf{P}(t) = n\,\mathrm{tr}_S\{\hat{\rho}^{(1)}(t)\hat{\boldsymbol{\mu}}\} = \frac{\mathrm{i}}{\hbar}n\int_{\infty}^{t}\mathrm{d}\tau\;\chi^{(1)}(t,\tau)\,\mathbf{E}(\tau) \tag{C2}$$

If we also take into consideration $\mathcal{U}(\tau-t_0)\hat{\rho}_{\mathrm{eq}} = \hat{\rho}_{\mathrm{eq}}$ (the equilibrium value of the density operator does not change in time), the used formula for the dipole−dipole correlation function, eq 17, results.

APPENDIX D: ABSORPTION LINE SHAPE IN THE EXCITON REPRESENTATION

The absorption line shape is calculated for the case of equally oriented SC−MNP systems. Accordingly, eq 23 takes the form

$$I(\omega) = Re\int_0^\infty \mathrm{d}t\;\mathrm{e}^{\mathrm{i}\omega t}\Big(\sum_\alpha d_\alpha^*\sum_j n_j\sigma_{\alpha g,j}(t) + \sum_N d_N^*\sum_j n_j\sigma_{Ng,j}(t)\Big) \tag{D1}$$

The summation with respect to the different molecules in the SC has been replaced by the one with respect to the exciton levels and we used $d_\alpha = [\mathbf{d}_\alpha\mathbf{n}]$ and $\sigma_{\alpha g,j}(t) = \langle\phi_\alpha|[\mathbf{e}_j\hat{\boldsymbol{\sigma}}(t)]|\phi_g\rangle$ (the $\mathbf{e}_j$ are unit vectors of a Cartesian coordinate system).

To achieve an analytical expression for the absorption line shape, we change to coherence related Green's functions

$$G_{\alpha g,j}(t) = -\mathrm{i}\theta(t)\,\sigma_{\alpha g,j}(t) \tag{D2}$$

dx.doi.org/10.1021/jp305505c | J. Phys. Chem. A 2012, 116, 11330−11340

and

$$G_{Ng,j}(t) = -i\theta(t)\,\sigma_{Ng,j}(t) \tag{D3}$$

Respective Fourier-transformed expressions give the absorption line shape, eq D1, as

$$I(\omega) = -\mathrm{Im}\Big(\sum_{\alpha} d_{\alpha}^{*} \sum_{j} n_j G_{\alpha g,j}(\omega) + \sum_{N} d_{N}^{*} \sum_{j} n_j G_{Ng,j}(\omega)\Big) \tag{D4}$$

Fourier-transformed equations of motion for the Green's functions follow as (cf. section IIE)

$$(\omega - \tilde{\omega}_{\alpha}) G_{\alpha g,j}(\omega) = d_{\alpha j} + \sum_{N} v_{\alpha N} G_{Ng,j}(\omega) \tag{D5}$$

and

$$(\omega - \tilde{\omega}_{N}) G_{Ng,j}(\omega) = d_{Nj} + \sum_{\alpha} v_{N\alpha} G_{\alpha g,j}(\omega) \tag{D6}$$

Introducing the self-energy matrix

$$\Sigma_{\alpha\beta}(\omega) = \sum_{N} \frac{v_{\alpha N} v_{N\beta}}{\omega - \tilde{\omega}_{N}} \tag{D7}$$

a closed equation for $G_{\alpha g,j}$ is obtained

$$(\omega - \tilde{\omega}_{\alpha}) G_{\alpha g,j}(\omega) = d_{\alpha j} + \sum_{N} \frac{v_{\alpha N} d_{Nj}}{\omega - \tilde{\omega}_{N}} + \sum_{\beta} \Sigma_{\alpha\beta}(\omega)\, G_{\beta g,j}(\omega) \tag{D8}$$

The absorption line shape can be written as

$$I(\omega) = -\mathrm{Im} \sum_{\alpha} \left(d_{\alpha}^{*} + \sum_{N} \frac{d_{N}^{*} v_{N\alpha}}{\omega - \tilde{\omega}_{N}} \right) \sum_{j} n_j G_{\alpha g,j}(\omega) - \mathrm{Im} \sum_{N} \frac{|d_N|^2}{\omega - \tilde{\omega}_{N}} \tag{D9}$$

An analytical expression of the line shape can be obtained if we neglect in eq D8 off-diagonal elements of $\Sigma_{\alpha\beta}(\omega)$. It results eq 24 discussed in the main text.

Considering a spherical MNP, where the plasmon excitations can be counted by multipole indices, the transition dipole moment d_{lm} is different from zero only for $l = 1$. Consequently, only dipole plasmon excitations contribute to the exciton dipole renormalization whereas all multipole plasmons participate in the exciton energy shift and broadening.

AUTHOR INFORMATION

Corresponding Author

*E-mail: may@physik.hu-berlin.de.

Notes

The authors declare no competing financial interest.

ACKNOWLEDGMENTS

V.M. thanks Joern Manz for the longstanding and fruitful scientific contacts in particular in the framework of Sfb 450 *Analysis and Control of Ultrafast Photoinduced Reactions* supported by the *Deutsche Forschungsgemeinschaft* from 1998 to 2010. Current financial support by the *Deutsche Forschungsgemeinschaft* through Sfb 951 (Y. Zelinskyy) and by the *China Scholarship Council* (Y. Zhang) is also gratefully acknowledged.

REFERENCES

(1) Heller, E. J. *Acc. Chem. Res.* **1981**, *14*, 368.
(2) May, V.; O. Kühn, *Charge and Energy Transfer Dynamics in Molecular Systems*; Wiley-VCH: Weinheim, 2000, 2004, 2011.
(3) Neugebauer, F.; Malzahn, D.; May, V. *Chem. Phys.* **1995**, *201*, 151.
(4) Odom, T. W.; Schatz, G. C. Special issue: 2011 Plasmonics. *Chem. Rev.* **2011**, *11*, 3667.
(5) Halas, N. J. *Nano Lett.* **2010**, *10*, 3816.
(6) Bellessa, J.; Bonnand, C.; Plenet, J. C.; Mugnier, J. *Phys. Rev. Lett.* **2004**, *93*, 036404.
(7) Sugawara, Y.; Kelf, T. A.; Baumberg, J. J.; Abdelsalam, M. E.; Bartlett, P. N. *Phys. Rev. Lett.* **2006**, *97*, 266808.
(8) Cade, N. I.; Ritman-Meer, T.; Richards, D. *Phys. Rev. B* **2009**, *79*, 241404(R).
(9) Wiederrecht, G. P.; Wurtz, G. A.; Hranisavljevic, J. *Nano Lett.* **2004**, *4*, 2121.
(10) Uwada, T.; Toyota, R.; Masuhara, H.; Asahi, T. *J. Phys. Chem. C* **2007**, *111*, 1549.
(11) Fofang, N. T.; Park, T.-H.; Neumann, O.; Mirin, N. A.; Nordlander, P.; Halas, N. J. *Nano Lett.* **2008**, *8*, 3481.
(12) Eisele, D. M.; Berlepsch, H. v.; Böttcher, C.; Stevenson, K. J.; Vanden Bout, D. A.; Kirstein, S.; Rabe, J. P. *J. Am. Chem. Soc.* **2010**, *132*, 2104.
(13) Carmeli, I.; Lieberman, I.; Kraversky, L.; Fan, Z.; Govorov, A. O.; Markovich, G.; Richter, S. *Nano Lett.* **2010**, *10*, 2069.
(14) Myers Kelley, A. *Nano Lett.* **2007**, *7*, 3235.
(15) Pustovit, V. N.; Shahbazyan, T. V. *Phys. Rev. Lett.* **2009**, *102*, 077401.
(16) Pustovit, V. N.; Shahbazyan, T. V. *Phys. Rev. B* **2010**, *82*, 075429.
(17) Niles, E. T.; Roehling, J. D.; Yamagata, H.; Wise, A. J.; Spano, F. C.; Moule, A. J.; Grey, J. K. *J. Phys. Chem. Lett.* **2012**, *3*, 259.
(18) Holcman, J.; Al Choueiry, A.; Enderlin, A.; Hameau, S.; Barisien, T.; Legrand, L. *Nano Lett.* **2011**, *11*, 4496.
(19) Bai, F.; Sun, Z.; Wu, H.; Haddad, R. E.; Coker, E. N.; Huang, J. Y.; Rodriguez, M. A.; Fan, H. *Nano Lett.* **2011**, *11*, 5196.
(20) Marciniak, H.; Li, X.−Q.; Würthner, F.; Lochbrunner, S. *J. Phys. Chem. A* **2011**, *115*, 648.
(21) Kyas, G.; May, V. *J. Chem. Phys.* **2011**, *134*, 034701.
(22) Zelinskyy, Y. R.; May, V. *Chem. Phys. Lett.* **2011**, *511*, 372.
(23) Zelinskyy, Y. R.; May, V. *Nano Lett.* **2012**, *12*, 446.
(24) Zhang, W.; Govorov, A. O. *Phys. Rev. B* **2011**, *84*, 081405(R).
(25) Brack, M. *Phys. Rev. B* **1989**, *39*, 3533.
(26) Gerchikov, L. G.; Guet, C.; Ipatov, A. N. *Phys. Rev. B* **2002**, *66*, 053202.
(27) Weick, G.; Molina, R. A.; Weinmann, D.; Jalabert, R. A. *Phys. Rev. B* **2005**, *72*, 115410.
(28) Weick, G.; Ingold, G.-L.; Jalabert, R. A.; Weinmann, D. *Phys. Rev. B* **2006**, *74*, 165421.
(29) Connerade, J.−P.; Solovyov, A. V. *Phys. Rev. A* **2002**, *66*, 013207.
(30) Brack, M. *Rev. Mod. Phys.* **1993**, *65*, 677.
(31) Bertsch, G. F.; Feldmeier, H. *Phys. Rev. C* **1997**, *56*, 839.
(32) Hagino, K. *Phys. Rev. B* **1999**, *60*, R2198.
(33) Lamichhane, K.; Brack, M.; Winkler, P. *Int. J. Quantum Chem.* **2011**, *111*, 4363.